

Simulation of Acoustic Radiation of an AC Servo Drive Verified by Measurements

D. Franck^a, M. van der Giet^a, L. Burdet^b, R. Coleman^b, K. Hameyer^a

^aInstitute of Electrical Machines, RWTH Aachen University, Schinkelstraße 4, D-52062 Aachen, Germany,

^bETEL SA, Zone Industrielle, CH-2112 Môtiers, Switzerland,

Email: david.franck@iem.rwth-aachen.de

Abstract – Nowadays the determination of the acoustic radiation of electric machines is of particular interest. This paper presents an overview of the steps for the acoustic simulation of electrical machines relying on analytic and numeric methods. Analytic methods offer fast and reliable results, especially for frequencies and ordinal numbers of the electromagnetically excited force. Numerical approaches allow for a higher accuracy and separation of the various effects, which influence the acoustic radiation. In particular, amplitudes of electromagnetic force waves, the deformation of the mechanical structure and the acoustic radiation can be studied more detailed. Principally the choice of mechanical material parameters influences the accuracy of the simulation model. Therefore, a method for the determination of mechanical material parameters is presented. In the studied case the acoustic radiation of an AC servo drive is simulated and verified by measurements.

Introduction

Owing to the customers' demands the acoustic radiation is gaining more importance in the development of electrical machines. Therefore, accurate and automated simulation models are needed for the detailed study of the sources of the acoustic radiation. In this paper a multiphysics simulation method applying weak numeric coupling is applied. In this regards, a coupling of electromagnetic simulation to determine the exciting forces, a structural-dynamic simulation to calculate the displacement of the stator surface and an acoustic simulation to estimate the radiated sound pressure is established. To improve the accuracy and to reduce the simulation time of the structural-dynamic model the laminated stator iron core is homogenized. By experimental and numeric modal analysis the mechanical material parameters, Youngs' modulus and Poisson ration and shear modulus, are determined applying an optimization algorithm.

Electromagnetic simulation

The essential part of the multiphysics computation chain is the electromagnetic simulation since the electromagnetic field generates force waves acting on the stator tooth-heads. Due to the homogenous structure in axial direction of the investigated motor, a two dimensional finite element (FE) model is used. The flux density distribution is calculated for one revolution of the rotor with a mechanical rotation of one degree per time step. The resulting air gap field is modal decomposed by a 2D-DFT and can be described by a Fourier-series with the flux density amplitude $B_{i,j}$ of each flux density wave, the ordinal number ν_j , the frequency f_i and the phase angle $\varphi_{i,j}$ by:

$$B(x, t) = \sum_{i=-i_{\max}}^{i_{\max}} \sum_{j=1}^{j_{\max}} B_{i,j} \cdot \cos(2\pi f_i \cdot t - \nu_j \cdot x - \varphi_{i,j}) \quad (1)$$

Whereby i represents the frequency order and i_{max} is determined by the number of calculated time steps per period, and j represents the circumferential order, j_{max} is given by the number of flux density samples in the air gap. In contrast to the classical approaches the force density waves σ are determined applying a convolution of the flux density waves [1] described by equation (1). A representation of the numerical sampled force density waves as Fourier-series can be given:

$$\sigma(x,t) = \frac{1}{2\mu_0} \sum_{k=1}^{k_{max}} \sum_{l=1}^{l_{max}} \hat{\sigma}_{k,l} \cdot \cos(2\pi(f_k \pm f_l) \cdot t - (v_k \pm v_l) \cdot x - (\varphi_k \pm \varphi_l)) \quad (2)$$

With this approach, a decomposition of the force density waves into combinations of flux density waves is possible. In connection with classical analytic approaches [2]-[3] the components of this force density wave can be mapped to known sources. This method offers a detailed insight to the generation of the force density waves[1]. This modal decomposed force density waves are studied individually for each frequency and ordinal number. The simulated force density distribution reveal that a large number of excitations have the mode number two. In the following the resultant force density wave with the frequency equal to two times the pole number p und the circumferential mode $v = 2$ studied in more detail due to its large amplitude. The flux density distribution for one time step and this major force density wave σ and its decomposition in the three most important components σ_A , σ_B and σ_C is presented in Fig. 1. The dominant component σ_A can be traced back to a superposition of the combination of the flux density waves of stator winding- and rotor space harmonics, stator space harmonics and the reluctance field and stator space harmonics and reluctance field. The frequencies and ordinal numbers of the flux density waves, which generate σ_A are given in table 1.

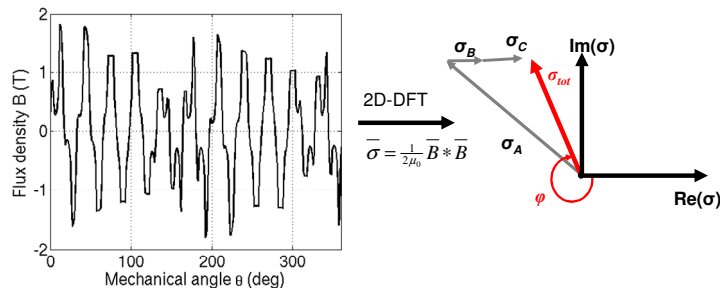


Fig. 1. Flux density distribution and decomposition of the force density wave with $f = 2pf_0$ and $v = 2$ of the investigated servo drive.

Table 1 Ordinal numbers and frequencies of important force density waves.

Cause	Circumferential ordinal number	Frequency order
stator winding space harmonics	$v = p \left(\frac{2mg}{N_q} - \xi \right), g = 0, \pm 1, \pm 2, \dots$	ξ
rotor space harmonics	$v = p(2k + 1), k = 0, \pm 1, \pm 2, \dots$	$2k + 1$
rotor reluctance field	$v = p(2l + 1) + N_1, l = 0, \pm 1, \pm 2, \dots,$	$2l + 2$

Material parameter optimization

With the calculated force densities acting on the stator teeth the deformation of the stator is to be calculated. Since the mechanical behavior of the stator depends on its material parameters a detailed knowledge of them is needed. A material homogenization is applied, since modeling of microstructures, such as the laminated iron core or resined coils, is memory and computation time expensive, especially for three dimensional FE models, which are needed for structural-dynamic simulation of complex structures. Furthermore, mechanical material parameters for structures, like laminated iron cores or resined coils, are not known in general. Therefore, the mechanical material parameters Young's modulus, Poisson ratio and shear modulus are determined based on numerical and experimental modal analysis. The laminated iron core as well as the resined coils is a transverse isotropic structure. These materials are characterized by symmetry in one plane, for example the x-y plane. Hooke's matrix for transverse isotropic materials with the given plane of symmetry is described by:

$$H = \begin{pmatrix} \frac{1}{E_x} & -\frac{\nu_{xy}}{E_x} & -\frac{\nu_{xz}}{E_x} & 0 & 0 & 0 \\ -\frac{\nu_{xy}}{E_x} & \frac{1}{E_x} & -\frac{\nu_{xz}}{E_x} & 0 & 0 & 0 \\ -\frac{\nu_{xz}}{E_x} & -\frac{\nu_{xz}}{E_x} & \frac{1}{E_z} & 0 & 0 & 0 \\ 0 & 0 & 0 & \frac{2(1+\nu_{xy})}{E_x} & 0 & 0 \\ 0 & 0 & 0 & 0 & \frac{1}{G_{yz}} & 0 \\ 0 & 0 & 0 & 0 & 0 & \frac{1}{G_{xz}} \end{pmatrix} \quad (3)$$

In this case the mechanical material properties can be described by five independent parameters, namely the Young's E_x and E_y in x and z direction, the shear modulus G_{yz} in the y-z plane and the Poisson ratio ν_{xy} and ν_{xz} in the x-y and the x-z plane. The homogenized parameters are determined solving an inverse numerical modal analysis, i.e. optimizing these parameters in order to fit the resonant frequencies of the numerical modal analysis to the results of the experimental ones. To solve this inverse problem Differential Evolution algorithm is applied [4]. The material parameters, their boundary constraints and relative deviation of the first four resonant frequencies of the laminated iron core as well as the material properties of bulk iron as comparison are given in table 2. The gained material parameters are used for the structural dynamic simulation.

Table 2 Optimized material parameters and deviation of the first 4 resonant frequencies.

Parameter	Laminated core	Bulk iron	Max	Min
E_x	212.7 GPa	210 GPa	250 GPa	100 GPa
E_y	26.3 GPa	210 GPa	100 GPa	1 GPa
ν_{xy}	0.40	0.3	0.6	0.2
ν_{xz}	0.14	0.3	0.6	0.01
G_{xy}	90.2 GPa	80 GPa	100 GPa	10 GPa
Resonant frequencies and relative deviation with material parameter optimization frequencies				
721 Hz	1947 Hz	1575 Hz	3553 Hz	
1,9 %	12.3%	0,4 %	1,6 %	

Structural-dynamic simulation

The structural-dynamic simulation is used to determine the deformation of the machine. In the FE model the deformation is represented by the displacements for each node. In the studied case the structural-dynamic simulation is done by numeric modal analysis, i.e. finding the eigenvalues of the corresponding eigen problem. Subsequent modal superposition is applied to determine the deformation for each frequency. For this purpose, a three dimensional model of the complete mechanical structure is built. The frequencies for the modal superposition are selected by amplitude of the force density wave and the eigenvalues of the numeric modal analysis. The surface-force densities for these frequencies are calculated from the flux density distribution using the Maxwell-stress tensor individually. In order to get the force distribution on the three dimensional model, the two dimensional force distribution is transformed from the 2-D electromagnetic mesh to the 3-D structure-dynamic mesh [5]. Fig. 2 shows the two dimensional force distributions and the three dimensional deformation as a result of the structural-dynamic simulation.

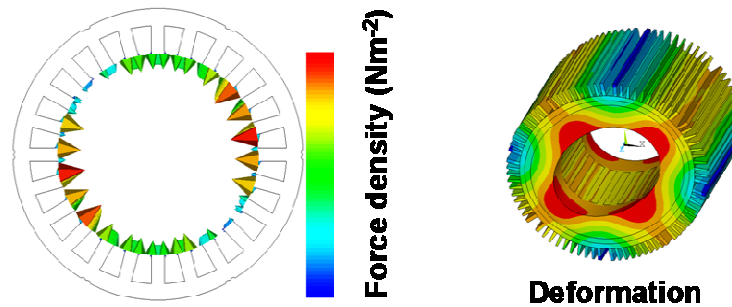


Fig. 2 Simulated force density and simulated deformation of the investigated motor.

Acoustic simulation

From the deformation the radiated sound pressure is calculated in a third step. This is done by converting the mechanical deformation to a velocity. Acoustic noise is the result of the air pressure alternation caused by the oscillation of the motors' surface. Therefore, only the oscillation of the surface has to be taken into account and the boundary element method (BEM) [5] is applied for the acoustic simulation. The basic principle is solving the Helmholtz differential equation to determine the sound pressure p :

$$\Delta \underline{p} + k^2 \underline{p} = 0 \quad (4)$$

Here is k the wave number defined by the fraction of angular frequency ω by the sound velocity c . Since BEM is applied a new model consisting of the outer surface mesh is build. The mechanical velocity is transformed to this mesh. The result of this simulation is the sound pressure and particle velocity on a half sphere around the motor with a distance of one meter. As a result the sound pressure distribution for the major excitation with $f = 2pf_0$ and $r = 2$ is presented in Fig. 3. The machine shows maxima of the radiated sound pressure in axial direction, whereby the front- and the backside represent minima of the radiation. These characteristics can be explained by the boundary condition of the simulation in the front side and the absence of an end bell on the backside.

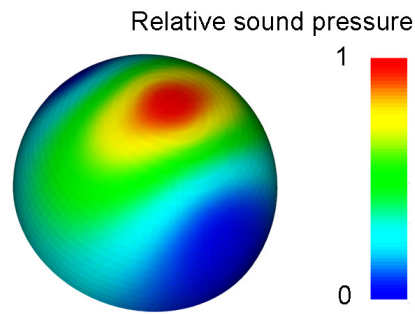


Fig. 3. Normalized sound pressure.

Results and validation by deformation measurements

The results of the simulation are the force distribution acting on the stator teeth, the deformation of the stator and the radiated sound pressure. For the structural-dynamic simulation the fitted material parameters are used. In this paper the simulation results of the deformation simulation are validated by measurements. Therefore, deformation measurements are performed. The acceleration is measured on the surface of the electrical machine at 16 points. Fig. 4 shows the design of the experiment. The acceleration is measured using a dual channel signal analyzer. One of the two accelerometers is kept at a constant position. The second sensor is moved around the surface of the machine. By double integration of the acceleration a the displacement d at the points is calculated

The result of the structural-dynamic simulation is validated by these measurements. The displacement on the surface of the three dimensional FE model is read at the measured positions. The deformation shape and the amplitudes for first eight mode numbers are compared. As an example the deformation at the major excitation with $f = 2pf_0$ is presented in Fig. 5. As expected from the force excitation the mode number of the deformation is $r = 2$. The measurements reveal comparable high amplitude with the mode number one. The reason for this may be an eccentricity, for example caused by an eccentric rotor adjustment, or magnetic eccentricity. Since the frequency of the deformation with mode number one is $f = 2pf_0$ the eccentricity is static. Hints for a static eccentricity are also found in the other frequency components of the measurements. The agreement of the simulation model with measurements tends to decrease with higher frequencies, but is still in satisfactory range.

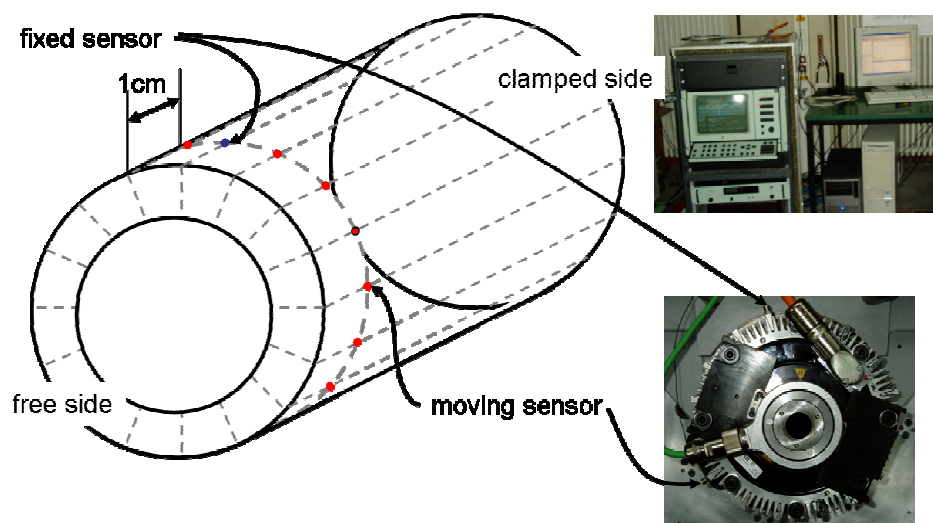


Fig. 4. Experiment setup for acceleration measurements.

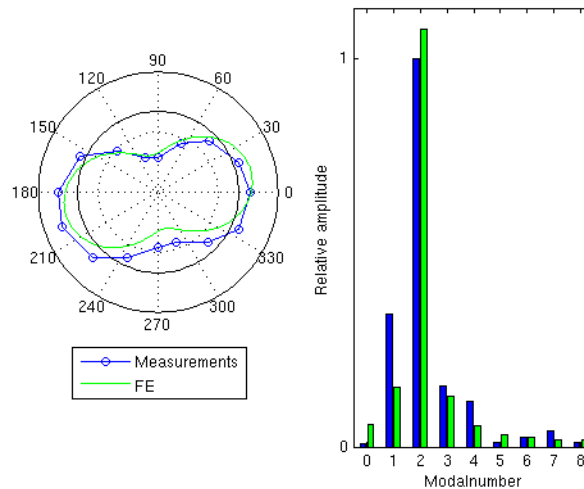


Fig. 5. Comparison of simulation and measurement: Displacement on the surface of the stator with $f = 2pf_0$.

Conclusions

In this paper, the electromagnetic excited body-sound and air-borne noise of an AC servo drive is analyzed. An automated multiphysics simulation model applying weak numerical coupling is presented and the important aspects for audible noise simulation of electrical machines pointed out. In particular the analysis of the electromagnetic forces is discussed. In contrast to commonly used standard mechanical material parameters a material homogenization is performed for the structural-dynamic simulation. The results of this simulation with the optimized material parameters are in good agreement with the measurements. Especially for the lower frequency range an error below 10% is gained. The accuracy of the model decreases with increase of the frequency. The simulation model reveals a realistic pattern of the body sound and acoustic radiation. Therefore, it is possible to benchmark the acoustic behavior of new designs before building a prototype.

References

- [1] M. van der Giet, R. Rothe, K. Hameyer, Asymptotic Fourier decomposition of tooth forces in terms of convolved air gap field harmonics for noise diagnosis of electrical machines, International Symposium on Numerical Field Calculation in Electrical Engineering, IGTE 2008, CD-Rom, 2008.
- [2] J. Gieras, C. Wang, and J. C. Lai, Noise of Polyphase Electric Motors. CRC Press Taylor&Francis Group, 2006.
- [3] Gieras, J.F.; Chong Wang; Joseph, C.S.L.; Ertugrul, N., Analytical Prediction of Noise of Magnetic Origin Produced by Permanent Magnet Brushless Motors, Electric Machines & Drives Conference, 2007. IEMDC '07. IEEE International, vol.1, no., pp.148-152, 3-5 May 2007.
- [4] Price, K. and Storn, R., Differential Evolution: Numerical Optimization Made Easy, Dr. Dobb's Journal, April 97, pp. 18 - 24.
- [5] M. Furlan, A. Cernigoj, and M. Boltezar, A coupled electromagnetic-mechanical-acoustic model of a DC electric motor, Int. J. Comput. Math. Electr. Electron. Eng., vol. 22, no. 4, 2003.